AJRCCM Articles in Press. Published on 09-November-2015 as 10.1164/rccm.201507-1281OC

Morphometric analysis of explant lungs in cystic fibrosis.

Mieke Boon[1*], Stijn E. Verleden[2*], Barbara Bosch[1*], Elise J. Lammertyn[2], John E. McDonough[2], Cindy Mai[3], Johny Verschakelen[3], Mariette Kemner-van de Corput[4], Harm A.W. Tiddens[4], Marijke Proesmans[1], Francois L. Vermeulen[1], Erik K. Verbeken[5], Joel Cooper[6], Dirk E. Van Raemdonck[2], Marc Decramer[2], Geert M. Verleden[2] , James C. Hogg[7], Lieven J. Dupont[2], Bart M. Vanaudenaerde[2], Kris De Boeck[1]

[1]Pediatric Pulmonology and Cystic Fibrosis Unit, Department of Pediatrics, University Hospitals Leuven, Belgium

[2]KU Leuven - University of Leuven, Department of Clinical and Experimental Medicine, Laboratory of Pulmonology, Lung Transplant Unit, B-3000 Leuven, Belgium

[3]Department of Pulmonary Radiology, University Hospitals Leuven, Belgium.

[4]Department of Pediatric Pulmonology and Allergology, Department of Radiology, Erasmus MC Rotterdam, the Netherlands

[5]Department of Pathology, University Hospitals Leuven, Belgium

[6]Department of Thoracic Surgery University of Pennsylvania, Philadelphia, PA, USA

[7]University of British Columbia James Hogg Research Centre, St. Paul's Hospital, Vancouver, BC, Canada

*authors contributed equally

Corresponding author

Mieke Boon

Department of Pediatrics, Pediatric Pulmonology

University Hospital Leuven

Herestraat 49

3000 Leuven, Belgium

Tel 0032/16/34.38.20

Fax 0032/16/34.38.42

Email mieke.boon@uzleuven.be

Author's contribution:

Acquisition of the data or the analysis and interpretation of information: M.B., S.E.V., B.B., E.L., J.E.M., C.M., M.K-vdC., J.C., B.M.V., K.D.B.

Involvement in the conception, hypothesis delineation, and design of the study: S.E.V., E.K.V., M.D., G.M.V., J.V., H.T., M.P., F.L.V., J.C.H., B.M.V., L.J.D., K.D.B

Writing the article or substantial involvement in its revision before submission: M.B., B.B., E.L., S.E.V., B.M.V., K.D.B.

All authors approved the final version of the manuscript.

Support: S.E.V is a senior research fellow of FWO (grant 12G8715N)

Running head: Morphometric analysis of explant CF lungs.

Subject: 9.16 (Lung diseases, cystic fibrosis)

Word count: 3500 (3500 max)

At a glance commentary:

Scientific knowledge on the subject: Chronic inflammation leads to bronchiectasis and mucus plugging in end-stage CF.

What this study adds to the field: Using a combined approach with multidetector CT, microCT and histology, we quantified the extensive changes and remodeling in end-stage CF lungs that start from airway generation 6 down to the level of the terminal bronchioles.

This article has an Online Data Supplement, which is accessible from this issue's table of content online at www.atsjournals.org

AJRCCM Articles in Press. Published on 09-November-2015 as 10.1164/rccm.201507-1281OC

Abstract

Rationale: After repeated cycles of lung infection and inflammation, patients with cystic fibrosis (CF) evolve to respiratory insufficiency. Although histology and imaging have provided descriptive information, a thorough morphometric analysis of end-stage CF lung disease is lacking.

Objectives: To quantify the involvement of small and large airways in end-stage CF.

Methods: Multidetector CT (MDCT) and microCT were applied to 11 air-inflated CF explant lungs and 7 control lungs to measure, count and describe the airway and parenchymal abnormalities in end-stage CF lungs. Selected abnormalities were further investigated with thin section histology.

Measurements and main results: On MDCT, CF explant lungs showed an increased median (IQR) number (631 (511-710) vs 344 (277-349), p 0.003) and size of visible airways (cumulative airway diameter 217 (209-250) cm vs 91 (80-105) cm, $p < 0.001$) compared to controls. Airway obstruction was seen, starting from generation 6 and increasing to 40-50% of airways from generation 9 onwards. MicroCT showed that the total number of terminal bronchioles was decreased (2.9 (2.6-4.4)/ml vs 5.3 (4.8-5.7)/ml, $p<0.001$); 49% were obstructed and the cross sectional area of the open terminal bronchioles was reduced (0.093 (0.084-0.123) vs 0.179 (0.140-0.196) mm^2, $p<0.001$). On microCT, 41% of the obstructed airways re-opened more distally. This remodeling was confirmed on histological analysis. Parenchymal changes were also seen, mostly in a patchy and peribronchiolar distribution.

Conclusions: Extensive changes of dilatation and obstruction in nearly all airway generations were observed in end-stage CF lung disease.

Key words: cystic fibrosis, microCT, airway remodeling, airway obstruction

Abstract word count: 239

List of abbreviations

CF	cystic fibrosis
CF-CT	cystic fibrosis chest tomography
IQR	interquartile range
FEV_1	forced expiratory volume in 1 second
FEF_{25-75}	forced expiratory flow between 25 and 75% of the expired volume
FEF_{75}	forced expiratory flow at 75% of the expired volume
FVC	forced vital capacity
Lm	mean linear intercept
MDCT	multidetector CT
RV	residual volume
SALD	severe advanced lung disease
T%	tissue percentage
TB	terminal bronchioles
TGV	total gas volume
TLC	total lung capacity

AJRCCM Articles in Press. Published on 09-November-2015 as 10.1164/rccm.201507-1281OC

VC	vital capacity

Introduction

Cystic fibrosis (CF) is a life-shortening disease with more than 90% of subjects dying from respiratory insufficiency (1).

The origins of CF lung disease are still not entirely understood. Abnormal mucus composition and secretion, defective mucociliary transport, reduced pH, impaired bacterial killing and excessive inflammatory responses probably all contribute to the initiation of lung disease (2). These early CF events quickly lead to structural lung damage, even in young children and in the absence of obvious clinical signs of lung disease (3). In the later disease stages, successive pulmonary exacerbations lead to progressive airway obstruction and increasingly severe structural lung damage with mucus impaction, bronchiectasis, atelectasis, hyperinflation and mosaic perfusion as main features (4, 5).

Thanks to several registry studies, the natural course of CF lung disease has been well described at the clinical, bacteriological and lung function level. Detailed information on lung remodeling is, however, lacking: imaging studies only provide indirect information about lung structure and lung histology samples are not easily obtained. An autopsy series of 82 children who died before the 1970s, describes disease progression: bronchitis, glandular hypertrophy, mucus plugging and bronchopneumonia are seen at all ages, but bronchiectasis is mainly seen in older children (6). A detailed histology/radiology correlation of 8 CF lungs from young adults who died in the 1970s, highlights focal areas of peribronchial pneumonia with necrosis and abscess formation, mostly surrounded by intact lung parenchyma and dilatation of central and peripheral airways (7). Some studies have examined the size and number of airways smaller than 2 mm in end-stage CF lungs (8-11). However, the results are

AJRCCM Articles in Press. Published on 09-November-2015 as 10.1164/rccm.201507-1281OC

not consistent, likely due to a difference in methods between studies and the lack of control lungs.

High resolution CT has been used to quantify histologically described abnormalities. However, the resolution of current *in vivo* imaging limits the study of the small airways.

Thus, although histology and imaging provide descriptive information on lung structure in CF, a thorough morphometric analysis of the CF lung is lacking. Recently, the development of microCT allows high resolution imaging and three dimensional viewing of the peripheral airways down to the level of the terminal bronchioles and alveoli (12, 13). A detailed description of CF lung pathology is indeed crucial to develop optimal treatment strategies. Our aim was therefore to combine multidetector CT (MDCT) and microCT to measure, count and describe the airway and parenchymal abnormalities in end-stage CF lungs. In addition, abnormalities detected were further explored and correlated with histology sections.

Some of the results of these studies have been previously reported in the form of abstracts (14-20).

Methods

Patients

We examined the left lungs, explanted from 11 patients with CF who underwent lung transplantation at the University Hospital of Gasthuisberg Leuven (Belgium) between June 2010 and July 2012. Prior to surgery, informed consent to analyze these lungs had been obtained from all patients. Seven non-used donor lungs were used as controls. Reasons why

donor lungs were not used for lung transplants are described in **Online Supplement E1**. The local hospital's ethical committee approved this study (ML6385).

Baseline CF patient characteristics were retrieved from the patient files. Last available results for spirometry and plethysmography were included and expressed as % predicted (21, 22). Pre-operative chest CT scans were evaluated in random order with CF-CT score, a validated upgraded version of the Brody-II score, (23, 24) and with SALD score (25) (**Online Supplements E1**).

Preparation of lungs for MDCT and microCT

The lungs were air-inflated to total lung capacity (TLC), frozen solid in the fumes of liquid nitrogen, and scanned with MDCT, according to a previously reported protocol (12, 13) (more detailed descriptions of the material and methods can be found in **Online supplements E1**). After MDCT scanning, the lungs were cut in 2 cm thick slices. From each slice, cores with a diameter of 1.4 cm were excised and processed for microCT scanning.

MDCT scan analysis

The airway bifurcations were counted manually by scrolling through the MDCT scan and numbered from proximal to distal. The main stem bronchus was considered generation 1 and each subsequent bifurcation was counted as a new airway generation until the visibility of more distal generations was limited by the resolution of the MDCT (0.6 mm). The number of airways was calculated from the number of bifurcations. The diameter of each airway segment was measured at the level of the most pronounced dilatation, not to underestimate bronchiectasis. Cumulative airway diameter was calculated as the sum of all airway diameters per generation, to quantify the extent and severity of bronchiectasis. Airway

AJRCCM Articles in Press. Published on 09-November-2015 as 10.1164/rccm.201507-1281OC

obstructions were defined as complete loss of the airway lumen, with no visible re-opening of the lumen downstream of the obstruction (**Figure 1**).

MicroCT scan analysis

The microCT resolution of 16.8 µm allowed to count and measure terminal bronchioles (TB) present in a lung core with a known volume. The TB represent the last generation of airways with a circumferential wall, before alveolar buds become visible. They represent the entrance to the pulmonary acinus and the point of transition from convection to diffusion of gasses in the lung. The number of TB/mL tissue were counted and the diameter/cross-sectional area of each TB was measured at their most distal point before evolution to respiratory bronchioles.

The parenchyma of lung cores of CF was compared to that of control lungs and was described in a qualitative way. The mean linear intercept (Lm), the mean distance between alveolar walls and thus a measure of emphysema, and parenchymal tissue volume (T%), a measure of fibrosis, were quantified.

The patency of TB and more proximal airways present in the microCT core was explored by following their path through the core.

Histology

Selected cores with specific features of interest on microCT (e.g. obstruction) were processed for histological analysis (**Online Supplement E1**).

Statistics

Because of low numbers, non-parametric statistics were used. Results were expressed as median (IQR).

Comparison between groups was performed by Mann Whitney test for continuous variables or Fisher's exact test for categorical variables. Correlations between parameters were assessed with Spearman correlation coefficients. All statistical analyses were performed with IBM SPSS Statistics 21.0. A p-value <0.05 was considered statistically significant.

MB and BB were trained to perform lung morphometric analysis and their results were validated against experienced readers (SEV and JM).

Results

Patient characteristics are reported in **Table 1**. Patients with CF were significantly younger ($p < 0.001$), shorter ($p = 0.008$) and lighter ($p < 0.001$) than control subjects. Pre-transplant lung function in CF showed very severe airway obstruction (low FEV_1 and FEV_1/FVC) and air trapping as indicated by high residual volume (RV). CT analysis showed that CF lungs had smaller volumes than the control lungs ($p = 0.004$), but were heavier ($p = 0.015$) and thus had a higher density ($p < 0.001$) (**Table 2**).

When comparing airway diameters between CF and control, the shorter stature and smaller lung volume could be possible confounders. Therefore, in MDCT analysis, the airway diameters of CF and control lungs are reported as corrected airway diameter (airway diameter/left lung volume).

The results for CF-CT and *ex vivo* and *in vivo* SALD scores of the left lung are shown in **Table Online Supplement E2**.

AJRCCM Articles in Press. Published on 09-November-2015 as 10.1164/rccm.201507-1281OC

MDCT

In CF, the number of visible airway bifurcations was increased compared to controls (631 (511–710) vs 344 (277–349), p = 0.003), there was a significant increase in corrected airway diameter per airway generation (p = 0.01) (**Table 2 and Figure 2a and 2b**) and in cumulative airway diameter per lung (217 cm (168–306) vs 91 cm (80–105), p < 0.001) (**Figure 2c**). Compared to control lungs, the number of visible airways was increased from airway generation 9 on and the diameter was increased from generation 6 on. A median of 35% (26–43) of airways per lung was obstructed, with obstructions starting from airway generation 6 and increasing to 50% in the more peripheral airways (**Figure 2d**). In control lungs, obstruction of airways was not observed.

The number of visible large (≥2 mm) and small airways (< 2 mm) was increased. A total of 340 (184–413) large airways per lung were seen in CF versus 116 (67-124) in controls (p <0.001) and 811 (539–1134) small airways per lung in CF versus 562 (425–585) in controls (p = 0.055) (**Figure Online supplement E3**).

In control lungs, there was no different number of airways counted in the upper (134 (111-235) versus the lower lobe (166 (114-211) (p = 0.81). However, in CF, the total number of visible airways was lower in the upper lobe compared to the lower lobe (218 (132-265) vs 426 (246-578), p = 0.019). The total cumulative airway diameter did not differ between upper and lower lobe in controls (38.6 cm (28.1-41.6) vs 51.9 cm (30.4-64.9), p = 0.32) nor in CF (71.6 cm (62.3-130.9) vs 109.8 cm (85.4-209.5), p = 0.12). The percentage of obstructed airways was similar in upper and lower CF lobes (38.1% (30.2-44.4) vs 33.3% (26.6-40.4), p = 0.40).

In CF lungs, there was a positive correlation between the number of airway generations and the cumulative airway diameter (r 0.75, p = 0.008) and an inverse correlation with the percentage of obstructed airways (r -0.66, p = 0.026).

MicroCT and histology

Approximately 9 cores per lung were analyzed with microCT, resulting in a total of 67 cores from control and 100 from CF lungs. It must be noted that the very peripheral lung regions may be underrepresented, as explained in **Online Supplements E1**.

The median number of visible (open or obstructed) TB/ml was significantly reduced in CF versus control cores (2.9/ml, (2.6-4.4) vs 5.3/ml (4.8-5.7), p < 0.001) (**Table 2**). The median TB diameter and their median cross-sectional area were also diminished (217 µm (209-250) vs 349 µm (346-405), p < 0.001 and 0.093 mm² (0.084-0.123) vs 0.179 mm² (0.140-0.196), p < 0.001). Obstruction of TB was not seen in control cores. In CF, only 49% of the TB remained open over their entire course; 59% of obstructed TB were completely obstructed, in 41% the lumen reopened downstream of the obstruction before leading into an open respiratory bronchiole **(Figure 3)**. The number of open TB/ml was thus significantly reduced in CF versus controls (2.6/ml (1.5-3.2) vs 5.3/ml (4.8-5.7), p < 0.001).

In the 100 CF cores, 466 airways with lumen obstruction were identified. In 389 (83%), the lumen remained obstructed and the airway appeared to disappear downstream of the obstruction (**Video Online Supplement E4**). In the remaining 77 airways (17%), the airway lumen restored downstream of the obstruction, albeit with a significantly decreased diameter (493 µm (351-923) upstream vs. 188 µm (122-255) downstream of the obstruction, p < 0.0001). The median length of the obstructed segments was 1.81 mm (1.357-2.77). A representative lesion is shown in **Online Supplement E5**. Matched histological examination

AJRCCM Articles in Press. Published on 09-November-2015 as 10.1164/rccm.201507-1281OC

of this lesion (**Figure 4**) showed airway wall thickening and mucus plugging, recognizable by purple, intraluminal threads. When following this airway downstream on microCT and matched histological slices, we observed airway branching, decreasing of the lumen size until it disappeared. However, further downstream, this airway re-opened with a delineated airway wall and lumen (3D reconstruction **video Online Supplement E6).** Detailed staining of another obstructive lesion showed neo-angiogenesis in the destructed airway wall and replacement of the obstructed lumen by granulation tissue, characterized by the presence of thin type III collagen fibers (**Online supplement E7)**.

CF cores had an increased tissue% versus controls (42%, (26-46) vs 28% (26-29), $p < 0.001$). The Lm measurements of the analyzed cores did not differ between CF and controls (239 (222-256) in CF versus 230 (212-239) in controls, $p = 0.29$).

On microCT, the parenchyma had a heterogeneous appearance with sudden transitions between normal and abnormal regions, often delineated by thickened septa. Parenchymal lesions were mainly centered around the airways: e.g. fibrotic emphysema around bronchiectatic lesions; zones of scarring and atelectasis around bronchioli (**Figure 5)**.

Correlations between MDCT/microCT and spirometry/CT scores

The total number of airway obstructions on MDCT correlated with the RV (r 0.65, $p = 0.043$), but not with other lung function parameters. There was no correlation between the number of open TB/ml and any lung function parameter.

The total cumulative airway diameter correlated significantly with the CF-CT score and the bronchiectasis subscore (r 0.76, $p = 0.007$ and r 0.86, $p = 0.001$ respectively). The total cumulative airway diameter also correlated with the SALD *ex vivo* subscores

'infection/inflammation' (r 0.76, p = 0.007) and the subscore 'low attenuation' (r -0.66, p = 0.026). The number of visible airway generations and the percentage of airway obstructions did not correlate with CT scores.

Discussion

We conducted a thorough morphometric analysis of end-stage CF lungs and showed extensive changes in the conducting airways as well as in the TB, situated in the transition zone from convective flow to diffusion. In the conducting airways, as observed with MDCT, mainly from airway generation 6 on and thus from the level of bronchioli, dilatation and obstruction of up to 50% of airways per generation was seen. Due to a widespread dilatation, more airways were visible above the threshold of 0.6 mm (resolution of HRCT) and the number of visible airways increased. There is a wide variability between patients in the findings on HRCT, reflecting predominance of large bronchiectasis with pronounced destruction in some patients, and hyperinflation with small airways obstruction in other patients. MicroCT allowed the study of the TB, where dramatic reduction of the number of TB and especially open TB, was seen. The gateways to the lung acini where oxygenation takes place was more than halved compared to non-used donor lungs.

We have now quantitatively shown that CF affects the peripheral airways, as was already previously suggested by indirect findings on spirometry, multiple breath washout and imaging (26). This process starts early in CF lung disease since the increased visibility of airways on chest CT, possibly induced by their dilatation, has also been confirmed in children with CF and tends to increase with age (27, 28, 29). Together, this information points towards the need for better treatment of CF small airway disease.

AJRCCM Articles in Press. Published on 09-November-2015 as 10.1164/rccm.201507-1281OC

These changes in number and size of TB, the gateways to the lung acini where oxygenation takes place, must have extensive consequences for normal ventilation and oxygenation. Indeed, normal airway branching and airway size are strictly regulated so that air flow steadily slows down by a progressive increase in total airway surface area. The orderly progression of airway diameters assures convective airflow throughout the bronchial tree with minimal resistance and dead space volume following the laws of Hess and Murray (30). In this way, the flow velocity of the air in the distal bronchial tree will match the diffusion velocity in acinar airways (30, 31). Likewise, the exact size and design of the acinus is critical to allow for optimal oxygenation at rest and during exercise by gas diffusion (32). In CF, the lung damage mainly occurs in the airways, with the interstitium and alveoli appearing better preserved. Hence, one could speak of a dissociation between the defective ventilation and diffusion through the airways and the almost normal gas exchange membrane. In theory, gas exchange capacity is thus preserved in the distal periphery of the lung. Again, more efficient treatment of small airway disease has the potential to greatly improve outcome in CF.

We have also shown that many airways that are obstructed, remain obstructed over their entire course or disappear under the detection limit of MDCT, while others re-open following an obstruction. Given the widespread airway obstruction while areas of atelectasis are remarkably limited, extensive collateral ventilation must go on in the CF lungs, possibly via interbronchiolar pathways of Martin, bronchiole-alveolar communications of Lambert or the interalveolar pores of Kohn (33). Although certainly less effective than ventilation through airways and less important in healthy lungs, pulmonary interdependence is likely the main driver of collateral ventilation in the presence of airway obstruction and especially when areas of the lungs have preserved ventilation. This explains why hypoxia is only seen in terminal CF, despite very severe flow obstruction. These data also agree with previous

findings of extensive obstruction and air trapping on chest CT of patients with end stage CF lung disease (25).

Staining for collagen further confirms the presence of newly formed collagen fibers and neovascularisation in these areas of obstruction, as present in granulation tissue. The mechanism of these obstructions is not known but resembles our previous findings in lungs with bronchiolitis obliterans syndrome after lung transplantation, where airways more proximal to the terminal bronchioles were obstructed, re-opened down-stream giving rise to a normal number of terminal bronchioles (13). In CF, this phenomenon is seen down to the TB level.

Our morphometric findings in control lungs are in agreement with the previously suggested TB size (490 µm), alveolar size (162 µm) and number of branching generations (varying from 18 to 30) (30). The control and CF lungs were well-inflated before freezing and therefore the measured dimensions should reflect *in vivo* measurements. The similar findings on CT imaging using SALD score *in vivo* and later *ex vivo* also validate the complex technique of lung processing. Likewise, our findings in CF are in agreement with previous histology information of mainly peribronchial disease and the patchy distribution throughout the lung (7, 9, 34-36). Even with 40 years between the obtained samples, and with a vastly different treatment regimen, these main features are still prominently present.

The findings of our study are of high clinical relevance for the treatment of CF lung disease. The maintenance treatment of chronic CF lung infection and airway obstruction aims to improve airway clearance through inhalation of mucolytics, airway hydrators or dornase alpha as well as chest physiotherapy while combatting airway infection with inhaled antibiotics (37, 38). These drugs, however, are unlikely to reach the peripheral airway

AJRCCM Articles in Press. Published on 09-November-2015 as 10.1164/rccm.201507-1281OC

generations where airway obstruction is most prominent, while chest physiotherapy techniques have also little impact beyond the more central airways. Novel therapies already attempt to target the more peripheral airways by improving the deposition of nebulized drugs and inhaled dry powders (39), and prevention of airway destruction by dampening the local inflammation is another treatment goal (40). Targeting this peripheral airway disease in an early stage to prevent destruction seems appropriate.

MDCT and microCT have also been used to study other obstructive lung diseases: major differences in site and nature of airway obstruction exist between chronic obstructive pulmonary disease (COPD) (12) and rejection after lung transplant (13). In COPD, the number of visible airways is decreased from airway generation 6 on; in chronic rejection these are not decreased but obstructed airways appeared with decreasing airway diameter. Only in CF an increase of visible airways was determined, but the proportion of obstructed airways increased from generation 6 to generation 9 and then remained constant around 40-50% of visible airways. MicroCT analysis of COPD lungs demonstrated a reduction of 80% in number of TB and of cross sectional area of TB; lung rejection was characterized by a normal number and size of TB. In CF, the number of TB per ml and their cross sectional area decreased around 50%, confirming that CF is a small airways disease, encompassing the TB and continuing up to generation 6.

Several drawbacks of the study can be identified. The study group is small due to time consuming and labor intensive analysis, and a challenging recruitment of control lungs. Manual counting of airways on HRCT is time-consuming, but gives much more information on airway generations compared to a general impression of the number of airways, obtained by automated airway counting, as described by de Boer et al. (27). The technique of microCT

is promising, but due to very high irradiation doses not applicable *in vivo*. We thus cannot obtain information on earlier stages of lung disease as its use is limited to explant or cadaver lungs. Relatively small parts of the lungs were analyzed by microCT and the very peripheral lung regions may be underrepresented. However, most previous studies only used a single biopsy per lung, while we studied around 9 cores spread throughout each lung. However we may have missed other types of lesions, especially in the lung periphery adjacent to the pleura.

Age, weight and height differed between CF and controls and this hampered comparing airway dimensions. Yet the differences between controls and CF are so clear that including more samples is unlikely to change our findings. There is a gap in evaluation of airway generations with MDCT (reliable up to 600 μm visibility) and microCT (with resolution of 16.8 μm); only the latter allows a detailed view of TB and further downstream to the level of the alveoli. An adult lung is too large to fit entirely in the microCT scan. By exploring all the airways in the microcores, no matter what generation they were, we tried to overcome that problem and concluded that obstruction and destruction were present in all airway generations.

In conclusion, in end-stage CF lung disease, we have identified extensive airway dilatation and obstruction in all airway generations from generation 6 on with an enormous reduction in the number and size of TB, the entry to the gas exchange unit of the lung. This accounts for the difficulty in ventilation and oxygenation present in end stage lung disease. Further study is needed to examine how these lesions arise during the course of the disease and how therapy can be directed to prevent these obstructions.

AJRCCM Articles in Press. Published on 09-November-2015 as 10.1164/rccm.201507-1281OC

Acknowledgments

The authors thank Philippe Nafteux, Allesia Stanzi, Herbert Decaluwe, Paul de Leyn, and Hans Van Veer for providing explanted lungs.

Mark Elliot for technical assistance.

References

1. Boyle MP, De Boeck K. A new era in the treatment of cystic fibrosis: correction of the underlying CFTR defect. *Lancet Respir Med* 2013; 1: 158-163.

2. Stoltz DA, Meyerholz DK, Welsh MJ. Origins of cystic fibrosis lung disease. *N Engl J Med* 2015; 372: 351-362.

3. Mott LS, Park J, Murray CP, Gangell CL, de Klerk NH, Robinson PJ, Robertson CF, Ranganathan SC, Sly PD, Stick SM, Arest CF. Progression of early structural lung disease in young children with cystic fibrosis assessed using CT. *Thorax* 2012; 67: 509-516.

4. Loeve M, Gerbrands K, Hop WC, Rosenfeld M, Hartmann IC, Tiddens HA. Bronchiectasis and pulmonary exacerbations in children and young adults with cystic fibrosis. *Chest* 2011; 140: 178-185.

5. Goss CH, Burns JL. Exacerbations in cystic fibrosis. 1: Epidemiology and pathogenesis. *Thorax* 2007; 62: 360-367.

6. Bedrossian CW, Greenberg SD, Singer DB, Hansen JJ, Rosenberg HS. The lung in cystic fibrosis. A quantitative study including prevalence of pathologic findings among different age groups. *Hum Pathol* 1976; 7: 195-204.

7. Friedman PJ, Harwood IR, Ellenbogen PH. Pulmonary cystic fibrosis in the adult: early and late radiologic findings with pathologic correlations. *AJR Am J Rroentgenol* 1981; 136: 1131-1144.

8. Hamutcu R, Rowland JM, Horn MV, Kaminsky C, MacLaughlin EF, Starnes VA, Woo MS. Clinical findings and lung pathology in children with cystic fibrosis. *Am J Respir Crit Care Med* 2002; 165: 1172-1175.

9. Sobonya RE, Taussig LM. Quantitative aspects of lung pathology in cystic fibrosis. *Am Rev Respir Dis* 1986; 134: 290-295.

AJRCCM Articles in Press. Published on 09-November-2015 as 10.1164/rccm.201507-1281OC

10. Hogg JC, Williams J, Richardson JB, Macklem PT, Thurlbeck WM. Age as a factor in the distribution of lower-airway conductance and in the pathologic anatomy of obstructive lung disease. *N Engl J Med* 1970; 282: 1283-1287.

11. Tiddens HAWM, Koopman LP, Lambert RK, Elliott WM, Hop WCJ, van der Mark TW, de Boer WJ, de Jongste JC. Cartilaginous airway wall dimensions and airway resistance in cystic fibrosis lungs. *Eur Respir J* 2000;15:735-42.

12. McDonough JE, Yuan R, Suzuki M, Seyednejad N, Elliott WM, Sanchez PG, Wright AC, Gefter WB, Litzky L, Coxson HO, Pare PD, Sin DD, Pierce RA, Woods JC, McWilliams AM, Mayo JR, Lam SC, Cooper JD, Hogg JC. Small-airway obstruction and emphysema in chronic obstructive pulmonary disease. *N Engl J Med* 2011; 365: 1567-1575.

13. Verleden SE, Vasilescu DM, Willems S, Ruttens D, Vos R, Vandermeulen E, Hostens J, McDonough JE, Verbeken EK, Verschakelen J, Van Raemdonck DE, Rondelet B, Knoop C, Decramer M, Cooper J, Hogg JC, Verleden GM, Vanaudenaerde BM. The site and nature of airway obstruction after lung transplantation. *Am J Respir Crit Care Med* 2014; 189: 292-300.

14. Boon M, Bosch B, Verleden S, Lammertyn E, Goeminne P, Vanaudenaerde B, Van Raemdonck D, Verbeken E, Verleden G, Hogg J, Verschakelen J, Dupont L, De Boeck K. Peripheral airways disease in cystic fibrosis assessed on explant HRCT. Paper presented at: 8th European CF Young Investigator Meeting; 2014 Feb 19-21; Paris, France.

15. Bosch B, Boon M, Verleden S, Lammertyn E, Goeminne P, Vanaudenaerde B, Van Raemdonck D, Verbeken E, Verleden G, Hogg J, Verschakelen J, Dupont L, De Boeck K. MicroCT analysis of small airway involvement in cystic fibrosis. Paper presented at: 8th European CF Young Investigator Meeting; 2014 Feb 19-21; Paris, France.

16. Lammertyn E, Bosch B, Boon M, Verleden S, Goeminne P, Vanaudenaerde B, Verbeken E, Verschakelen J, Van Raemdonck D, Verleden G, Hogg J, De Boeck K, Dupont L. A histological and microCT study on small airways in end-stage cystic fibrosis lung disease. Paper presented at: 8th European CF Young Investigator Meeting; 2014 Feb 19-21; Paris, France.

17. Bosch B, Boon M, Verleden S, Lammertyn E, Goeminne P, Vanaudenaerde B, Van Raemdonck D, Verbeken E, Verleden G, Hogg J, Verschakelen J, Dupont L, De Boeck K. Small-airway disease in cystic fibrosis studied with Multidetector CT and microCT. *J Cyst Fibros* 2014;13:S69.
18. Lammertyn E, Bosch B, Boon M, Verleden S, Goeminne P, Vanaudenaerde B, Verbeken E, Verschakelen J, Van Raemdonck D, Verleden G, Hogg J, De Boeck K, Dupont L. Structural alterations in the end-stage cystic fibrosis lung: comparing histopathology to microCT. *J Cyst Fibros* 2014;13:S28.
19. Bosch B, Boon M, Verleden S, Lammertyn E, Goeminne P, Vanaudenaerde B, Van Raemdonck D, Verbeken E, Verleden G, Hogg J, Verschakelen J, Hogg J, Dupont L, De Boeck K. Lung units in cystic fibrosis studies with microCT. *Ped Pulmonol* 2014;49(Suppl S37):S46-47.
20. Boon M, Bosch B, Lammertyn E, Verleden S, Goeminne P, Vanaudenaerde B, Van Raemdonck D, Verbeken E, Verleden G, Hogg J, Verschakelen J, Dupont L, De Boeck K.Quantitative evaluation of CF airways using HRCT, µCT and histology *Eur Respir J* 2014;44:Suppl.58,3447.
21. Quanjer PH, Tammeling GJ, Cotes JE, Pedersen OF, Peslin R, Yernault JC. Lung volumes and forced ventilatory flows. Report Working Party Standardization of Lung Function Tests, European Community for Steel and Coal. Official Statement of the European Respiratory Society. *Eur Respir J* 1993; 16: 5-40.
22. Quanjer PH, Stanojevic S, Cole TJ, Baur X, Hall GL, Culver B, Enright PL, Hankinson JL, Ip MS, Zheng J, Stocks J. Multi-ethnic reference values for spirometry for the 3-95 year age range: the global lung function 2012 equations. *Eur Respir J* 2012; 40: 1324-43.
23. Wainwright CE, Vidmar S, Armstrong DS, Byrnes CA, Carlin JB, Cheney J, Cooper PJ, Grimwood K, Moodie M, Robertson CF, Tiddens HA. Effect of bronchoalveolar lavage-directed therapy on Pseudomonas aeruginosa infection and structural lung injury in children with cystic fibrosis: a randomized trial. *JAMA* 2011 Jul 13;306(2):163-71.

AJRCCM Articles in Press. Published on 09-November-2015 as 10.1164/rccm.201507-1281OC

24. Brody AS, Kosorok MR, Li Z, Broderick LS, Foster JL, Laxova A, Bandla H, Farrell PM. Reproducibility of a scoring system for computed tomography scanning in cystic fibrosis. *J Thorac Imaging* 2006; 21: 14–21.

25. Loeve M, van Hal PT, Robinson P, de Jong PA, Lequin MH, Hop WC, Williams TJ, Nossent GD, Tiddens HA. The spectrum of structural abnormalities on CT scans from patients with CF with severe advanced lung disease. *Thorax* 2009; 64: 876-882.

26. Tiddens HAWM, Donaldson SH, Rosenfeld M, Pare PD. Cystic fibrosis lung disease starts in the small airways: Can we treat it more effectively? *Ped Pulmonol* 2010; 45: 107-17.

27. deBoer EM, Swiercz W, Heltshe SL, Anthony MM, Szefler P, Klein R, Strain J, Brody AS, Sagel SD. Automated CT scan scores of bronchiectasis and air trapping in cystic fibrosis. *Chest* 2014; 145: 593-603.

28. Kuo W, de Bruijne M, Nasserinejad K, Ozturk H, Chen Y, Perez-Rovira A, Tiddens HAWM. Assessment of bronchiectasis in children with cystic fibrosis by comparing airway and artery dimensions to normal controls on inspiratory and expiratory spirometer guided chest computed tomography. *Insights Imaging* 2015; 6 Suppl: S197.

29. Kuo W, de Bruijne M, Ozturk H, Baoyue L, Perez-Rovira A, Tiddens HAWM. Sensitive and objective method to diagnose bronchiectasis on inspiratory and expiratory chest computed tomography in children with cystic fibrosis. *Ped Pulmonol* 2014; 49 Suppl:S366.

30. Weibel ER, Sapoval B, Filoche M. Design of peripheral airways for efficient gas exchange. *Respir Physiol Neurobiol* 2005; 148: 3-21.

31. Hou C, Gheorghiu S, Coppens M-O, Huxley VH, Pfeifer P. Gas Diffusion through the Fractal Landscape of the Lung: How Deep Does Oxygen Enter the Alveolar System? In: Losa GA, Merlini D, Nonnenmacher TF, Weibel ER, editors. Fractals in Biology and Medicine: Birkhäuser Basel; 2005. p. 17-30.

32. Sapoval B, Filoche M, Weibel ER. Smaller is better--but not too small: a physical scale for the design of the mammalian pulmonary acinus. *Proc Natl Acad Sci U S A* 2002; 99: 10411-10416.

33. Menkes H, Traystman R, Terry P. Collateral ventilation. *Fed Proc* 1979; 38: 22-26.

34. Wentworth P, Gough J, Wentworth JE. Pulmonary changes and cor pulmonale in mucoviscidosis. *Thorax* 1968; 23: 582-589.

35. Zuelzer WW, Newton WA, Jr. The pathogenesis of fibrocystic disease of the pancreas; a study of 36 cases with special reference to the pulmonary lesions. *Pediatrics* 1949; 4: 53-69.

36. Burgel PR, Montani D, Danel C, Dusser DJ, Nadel JA. A morphometric study of mucins and small airway plugging in cystic fibrosis. *Thorax* 2007; 62: 153-161.

37. Mogayzel PJ, Jr., Naureckas ET, Robinson KA, Mueller G, Hadjiliadis D, Hoag JB, Lubsch L, Hazle L, Sabadosa K, Marshall B. Cystic fibrosis pulmonary guidelines. Chronic medications for maintenance of lung health. *Am J Respir Crit Care Med* 2013; 187: 680-689.

38. Smyth AR, Bell SC, Bojcin S, Bryon M, Duff A, Flume P, Kashirskaya N, Munck A, Ratjen F, Schwarzenberg SJ, Sermet-Gaudelus I, Southern KW, Taccetti G, Ullrich G, Wolfe S, European Cystic Fibrosis S. European Cystic Fibrosis Society Standards of Care: Best Practice guidelines. *J Cyst Fibros* 2014; 13 Suppl 1: S23-42.

39. Tiddens HA, Bos AC, Mouton JW, Devadason S, Janssens HM. Inhaled antibiotics: dry or wet? *Eur Respir J* 2014 Nov; 44: 1308-18.

40. Cohen-Cymberknoh M, Kerem E, Ferkol T, Elizur A. Airway inflammation in cystic fibrosis: molecular mechanisms and clinical implications. *Thorax* 2013; 68: 1157-1162.

AJRCCM Articles in Press. Published on 09-November-2015 as 10.1164/rccm.201507-1281OC

Figure legends

Figure 1: Airway obstructions as seen on MDCT

1a: Obstructions in large airways in transversal MDCT section. A large saccular bronchiectatic airway with a 0.5 cm diameter (A) is partially filled with mucus (arrow) and is followed downstream (B-C). After branching (D, arrowhead), one bronchus suddenly narrows (G, arrow), becomes obstructed (H, arrow) and disappears (I). The other bronchus remains open (G-I), branches again (J, arrowhead), and once more one branch becomes obstructed and disappears (K-L, arrow), while the other branch remains open.

1b: Obstructions in distal airways in longitudinal sections. The lumen of a small, peripheral airway can clearly be discerned (arrow, M-N). However one section downstream shows the lumen gets filled (O), resulting in a closed lumen (arrowhead) which is not discernible any more with MDCT (P, arrowhead).

Figure 2: Results of MDCT scan analysis

2a: Airway diameter per airway generation in control and CF lungs. Data are shown as median and 95% CI. The median number of visible airways per generation is presented in the legend of the graph for CF and control lungs.

2b: Corrected airway diameter per airway generation in control and CF lungs. Data are shown as median and 95% CI. The median number of visible airways per generation is presented in the legend of the graph for CF and control lungs.

2c: The cumulative airway diameter (not corrected for lung volume) per generation in CF and control lungs. Data are shown as median and 95% CI. The median number of visible airways per generation is presented in the legend of the graph for CF and control lungs.

2d: The number of visible airways in control lungs and in CF lungs as seen with MDCT. More airways are visible in CF lungs, from generation 9 on. In control lungs there are no obstructed airways. In CF lungs, patent as well as obstructed airways are seen.

Figure 3: Terminal bronchiole on microCT imaging

Obstruction at the level of a terminal bronchiole. Panel A shows an overview of a lesion, starting proximally from a dilated airway (*) that becomes obstructed with mucus (arrowhead). The lumen reopens more distally at the level of the terminal bronchiole (TB), before giving rise to the respiratory bronchioles (RB). Panels B to I show transverse views from proximal to distal along this same airway track to unequivocally demonstrate airway obstruction and reopening distally. Intermittent reappearing of the airway lumen in panel D.

Figure 4: Validation of airway abnormalities on microCT by histology of same section

A bronchiectatic lesion (red arrowhead), with a diameter much larger than the accompanying vessel, is shown (blue arrow) (a). The lumen gets partially filled with mucus, while the lumen is getting smaller and smaller, resulting in an airway with no discernible lumen any longer. (b-d), Surprisingly, more distally from this completely occluded airway, we see that the airway bifurcates (g) with one branch re-opening with a smaller airway lumen (h), while the other remains obstructed (green arrowhead).

Figure 5: Parenchymal lesions as seen on microCT

(A) the thickened septum separates a zone with increased density of the interstitium from a zone with normal looking parenchyma and alveoli (N).

(B) peribronchiolar scarring with and dilatated emphysematous alveoli (*)

(C) zone of scarring and atelectasis centered around a bronchiolus (arrowhead)

AJRCCM Articles in Press. Published on 09-November-2015 as 10.1164/rccm.201507-1281OC

Tables

Table 1: Baseline characteristics of controls and patients with CF

		Controls	CF	p-value (Mann-Whitney or Fisher exact test)
	Number of subjects	7	11	
	Sex ratio M/F	5/2	4/7	0.34
	Age (years)	53 (43 -66)	22 (21 – 28)	< 0.001*
	Height (cm)	175 (170 – 180)	160 (153 – 172)	0.008*
	Weight (kg)	80 (65 – 85)	45 (41 – 57)	< 0.001*
	Pulmonary Function **% pred, median (IQR)**			
Spirometry	FVC	-	44 (35-53)	
	FEV_1	-	24 (18-29)	
	FEV_1/FVC	-	52 (47-57)	
	FEF_{25-75}		7 (5-8)	
	FEF_{75}		7 (6-7)	
Plethysmography	TLC	-	95 (81-102)	
	VC	-	54 (36-67)	
	RV	-	196 (167-257)	
	TGV	-	123 (115-149)	

Legend: results are given as N or median (IQR). Abbreviations: IQR interquartile range; FVC forced vital capacity; FEV_1 forced expiratory volume in 1 second; FEF_{25-75} forced expiratory flow between 25 and 75% of the expired volume; FEF_{75} forced expiratory flow at 75% of the expired volume; TLC total lung capacity; VC vital capacity; RV residual volume; TGV total gas volume; * statistically significant

Table 2: Results of *ex vivo* MDCT and microCT analysis

***Ex vivo* MDCT measurements (left lung)**	**Controls**	**CF**	**p-value (Mann-Whitney)**
Lung volume (L)	3.21 (2.91 – 3.63)	2.22 (1.96 – 2.46)	0.004*
Lung mass (g)	433 (399 – 474)	623 (493 – 784)	0.015*
Lung density (g/L)	137 (124 – 150)	241 (236 – 334)	< 0.001*
Cumulative airway diameter (cm)	91 (80-105)	217 (209-250)	< 0.001*
Airway bifurcations (n)	344 (277-349)	631 (511-710)	0.003*
Airway obstructions (%)	-	35 (28-43)	
***Ex vivo* microCT measurements**			
Number of visible TB (n/ml)	5.3 (4.8-5.7)	2.9(2.6-4.4)	< 0.001*
Number open TB (n/ml)	5.3 (4.8-5.7)	2.6 (1.5-3.2)	< 0.001*
Diameter of TB (µm)	349 (346-405)	217 (209-250)	< 0.001*
Cross-sectional area of TB (mm^2)	0.179 (0.140-0.196)	0.093 (0.084-0.123)	< 0.001*
Lm	230 (212-239)	239 (222-256)	0.285
Tissue%	28 (26-29)	42 (36-46)	< 0.001

Legend:

AJRCCM Articles in Press. Published on 09-November-2015 as 10.1164/rccm.201507-1281OC

Parameters are expressed as median and interquartile range. The *ex vivo* microCT parameters are based on the measurements in the selected cores. Because there may be underrepresentation of the peripheral lung regions, no assumptions on the whole lung can be made.

Abbreviations: MDCT multidetector CT ; TB terminal bronchiole; Lm mean linear intercept, * statistically significant by Mann Whitney U test.

Figures

Figure 1a

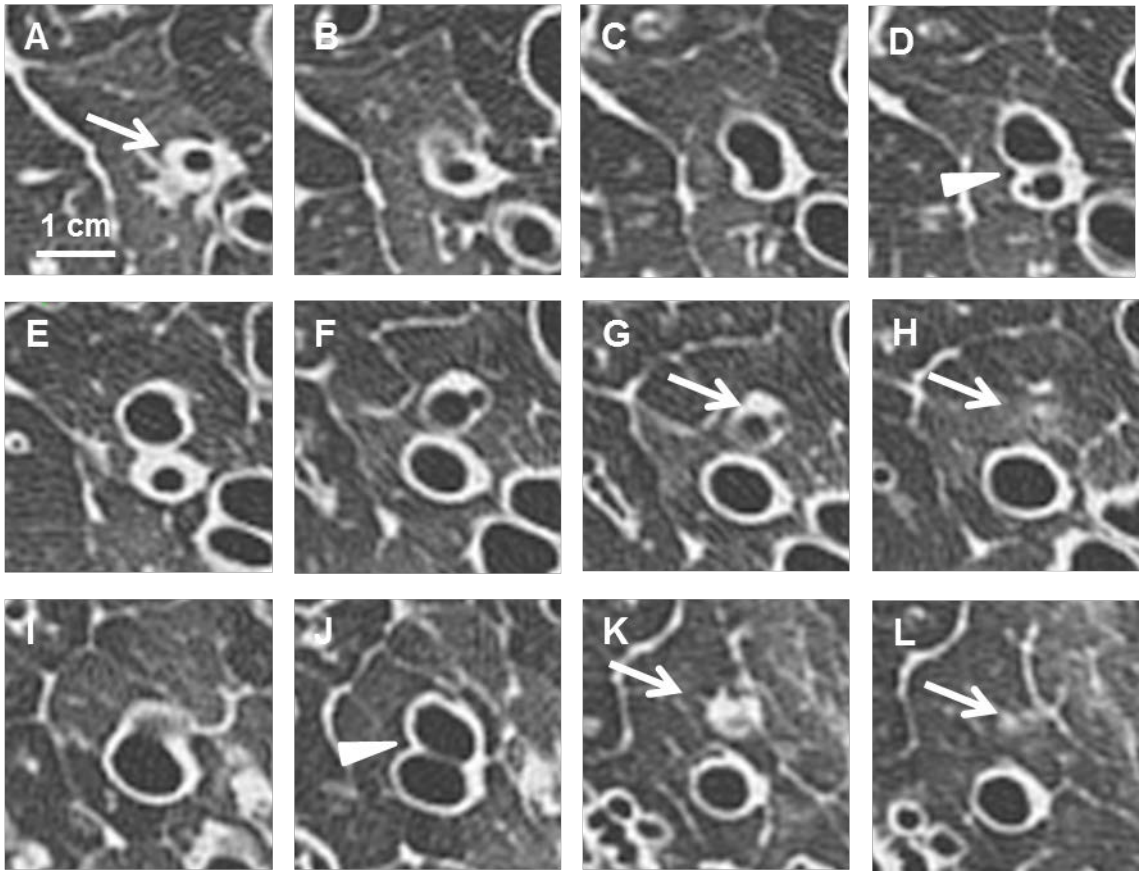

AJRCCM Articles in Press. Published on 09-November-2015 as 10.1164/rccm.201507-1281OC

Figure 1b

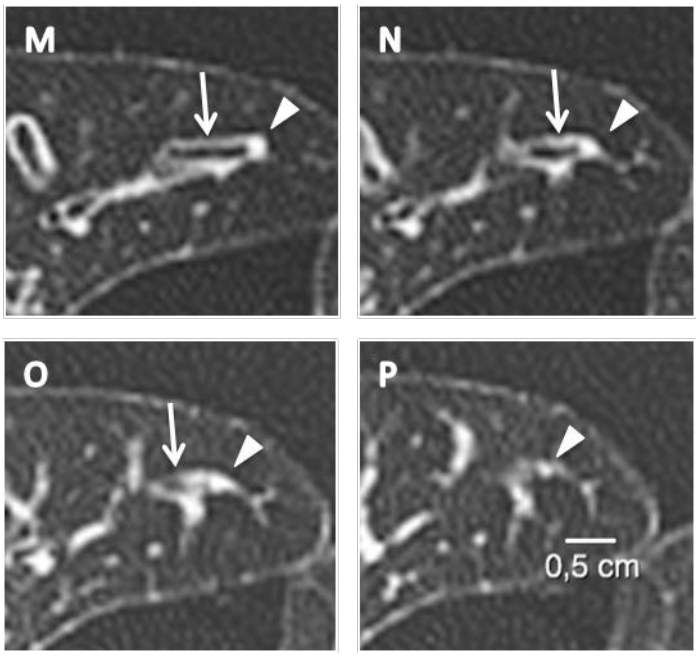

Figure 2

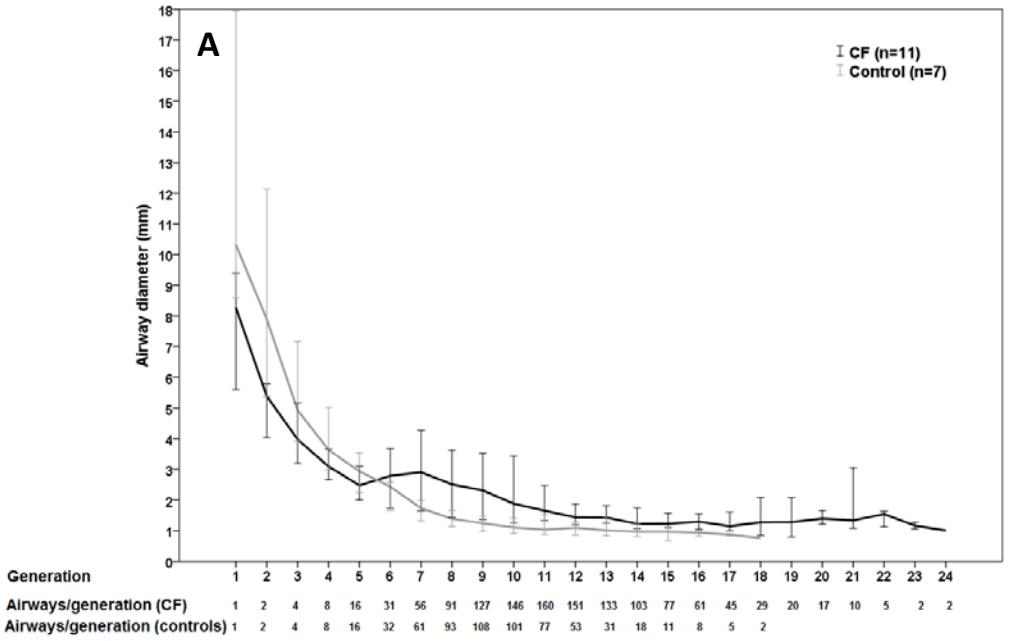

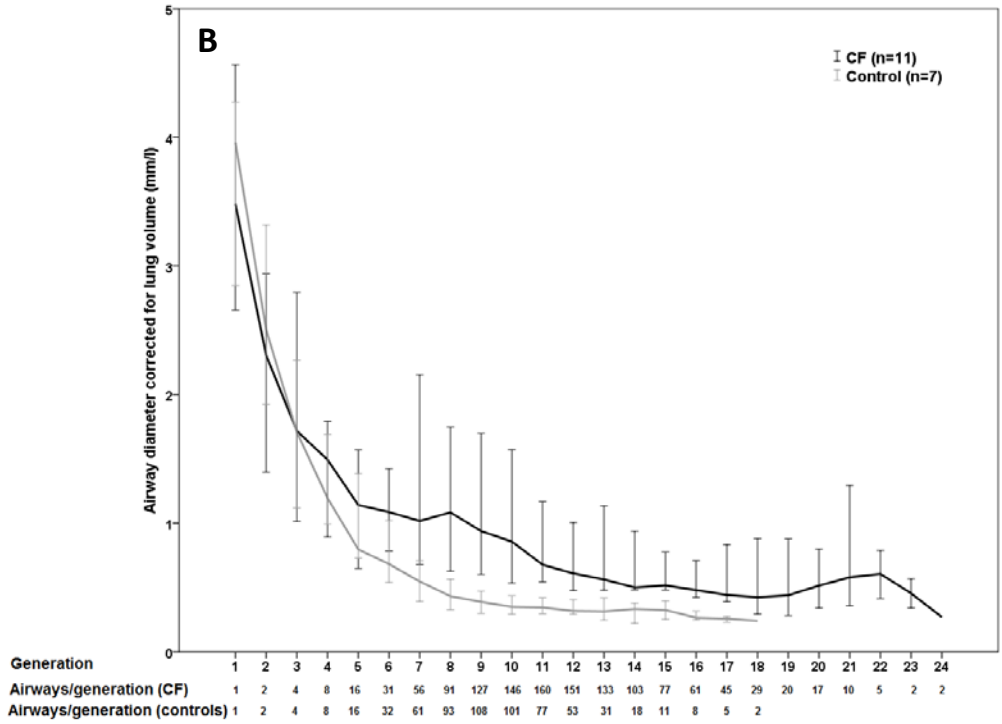

AJRCCM Articles in Press. Published on 09-November-2015 as 10.1164/rccm.201507-1281OC

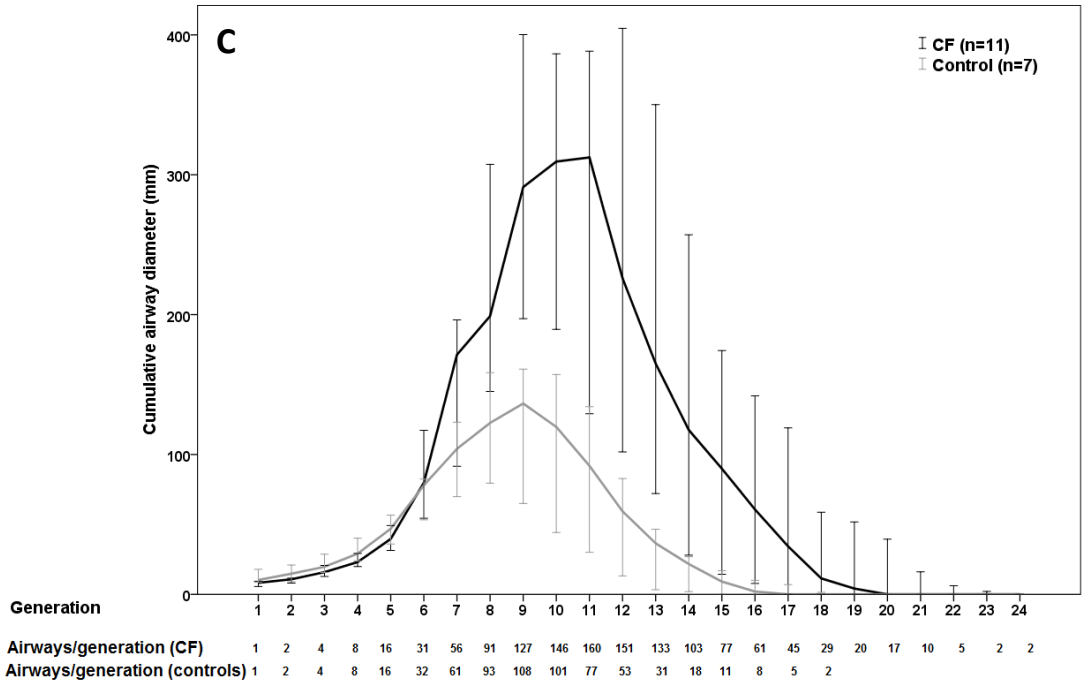

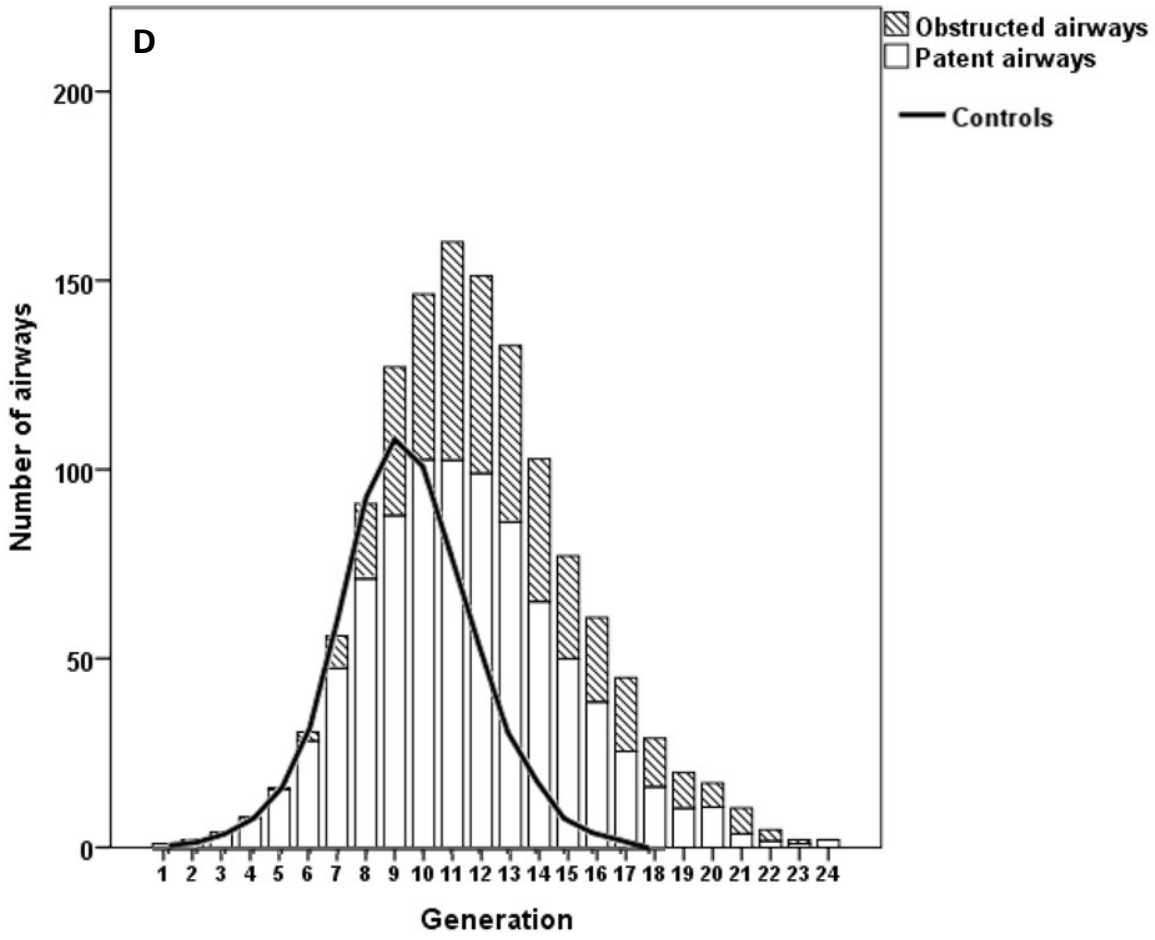

Figure 3

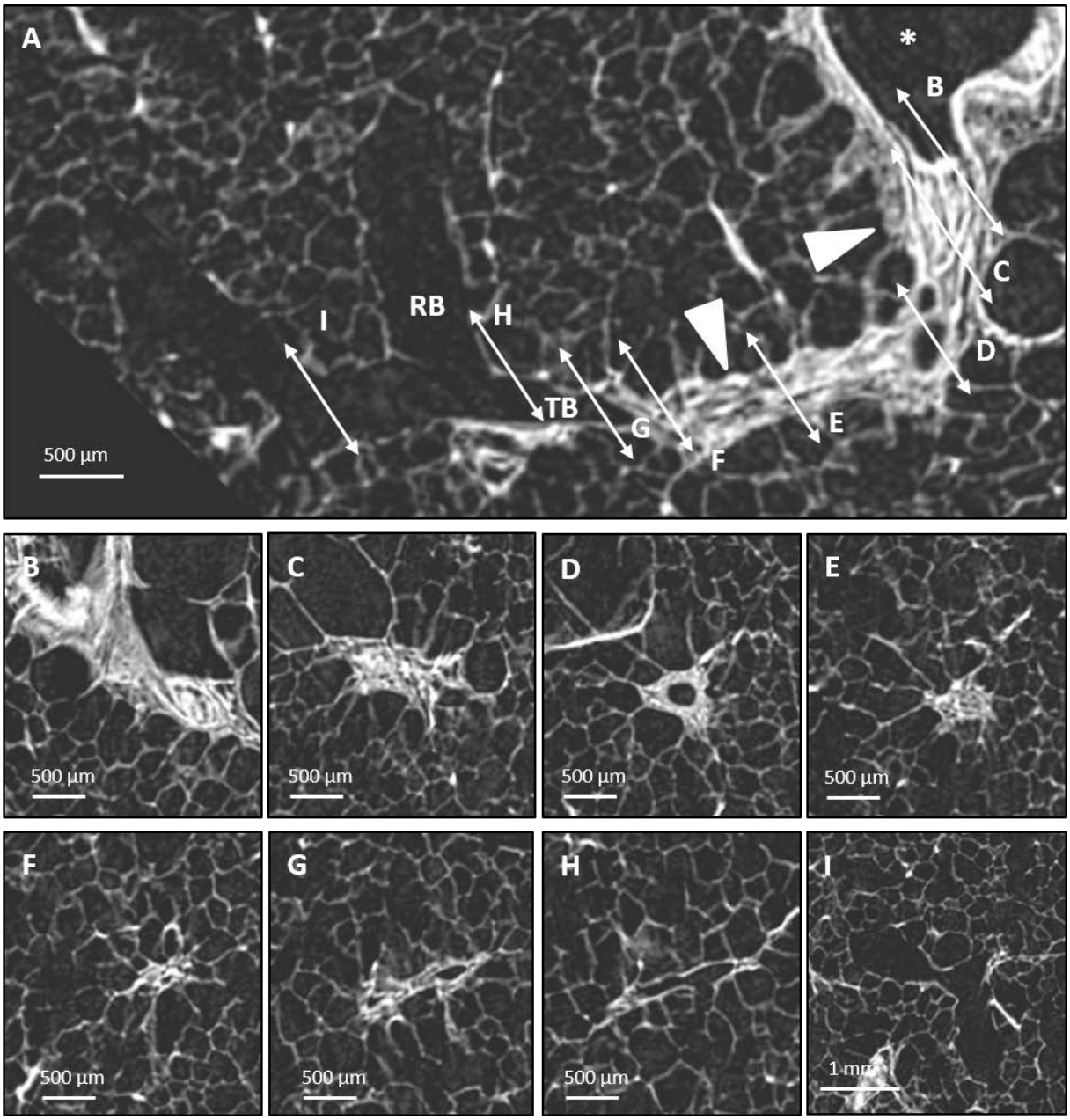

AJRCCM Articles in Press. Published on 09-November-2015 as 10.1164/rccm.201507-1281OC

Figure 4

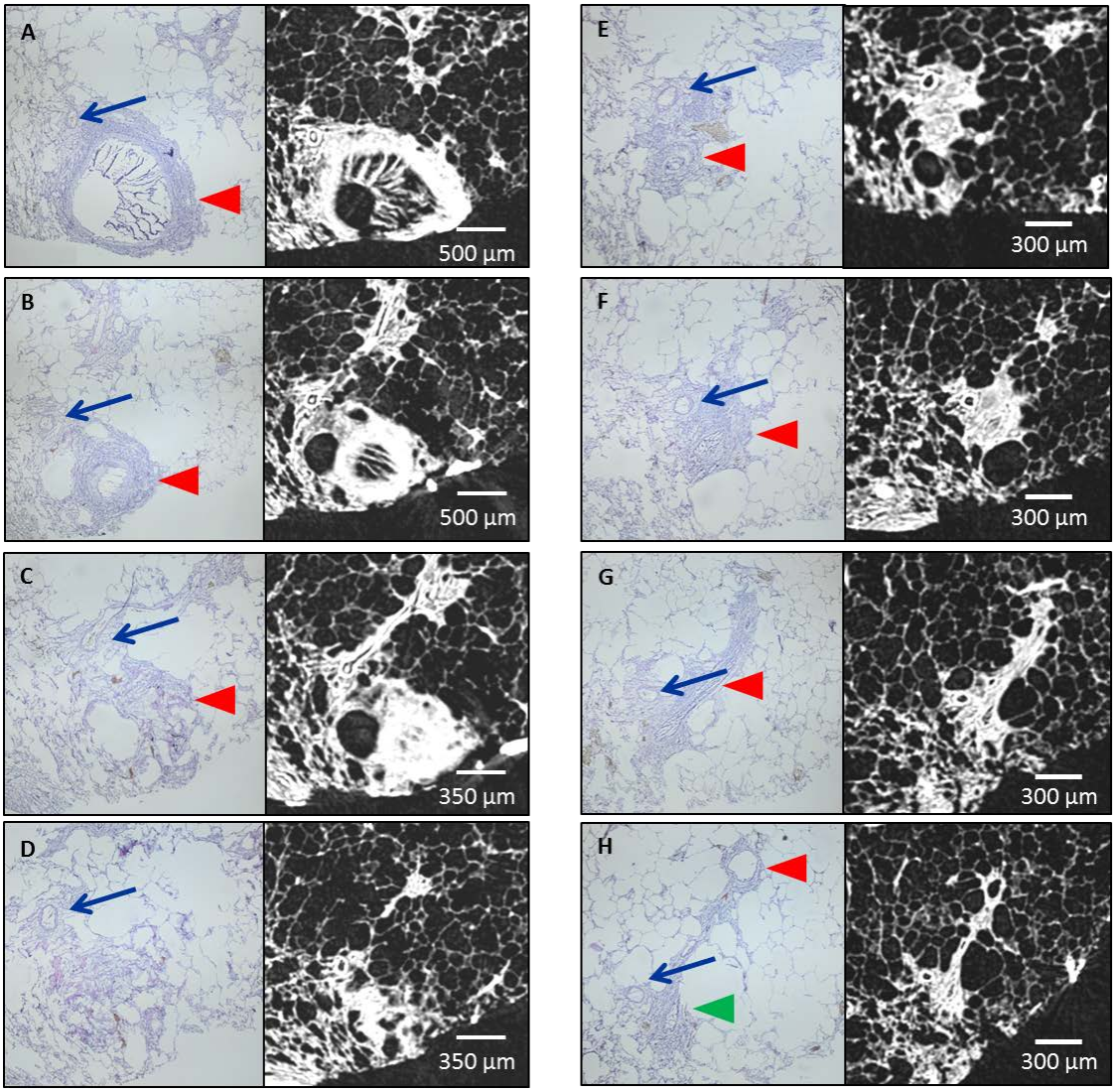

Figure 5

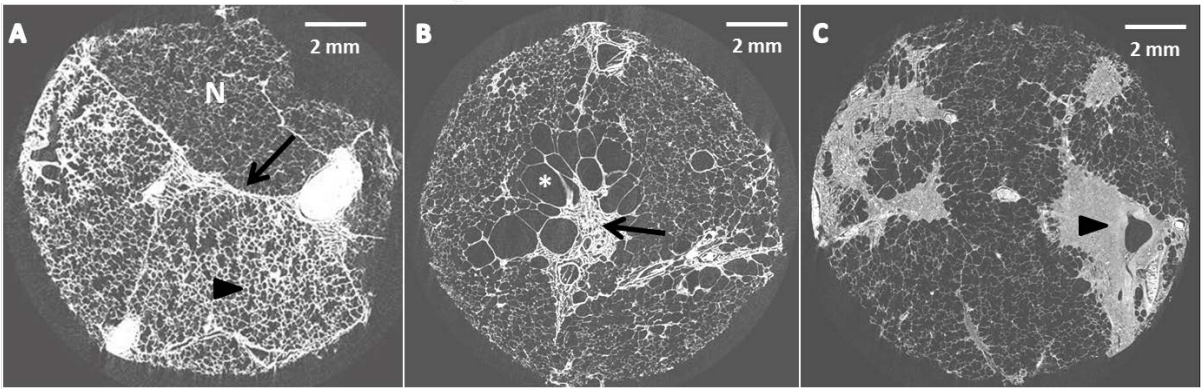

AJRCCM Articles in Press. Published on 09-November-2015 as 10.1164/rccm.201507-1281OC

Morphometric analysis of explant lungs in cystic fibrosis.

Mieke Boon[1*], Stijn E. Verleden[2*], Barbara Bosch[1*], Elise Lammertyn[2], John E. McDonough[3], Cindy Mai[4], Johny Verschakelen[4], M Kemner-van de Corput[5], Harm Tiddens[5], Marijke Proesmans[1], Francois L. Vermeulen[1], Erik K.Verbeken[6], Joel Cooper[7], Marc Decramer[2], Geert M. Verleden[2,8], James C. Hogg[9], Lieven J. Dupont[2,8], Bart M. Vanaudenaerde[2], Kris De Boeck[1]

ONLINE DATA SUPPLEMENT

Online Supplement E1: Methods

Patient material and information

Reasons for ineligibility of the control lungs as donor lungs consisted of: 'receptor could not be allocated within timeframe' (n=3), 'receptor died before the lungs could be engrafted' (n=1), 'renal tumor was detected at the moment of prelevation' (n=1), 'persistent embolization' (n=1) and 'low donor paO_2' (n=1). Organs were obtained at the University Hospital Gasthuisberg (n=4) and from the Organ Donor Program of the Gift of Life organization in Philadelphia (n=3). Informed consent was obtained from the donors' next of kin or was presumed according to the Belgian law that allows the use of organs for donation or research, unless a person explicitly decides to 'opt out'.

CT scoring

CF-CT scoring was performed by a validated scorer, MB (validation through on-line training module of corelab LungAnalysis Rotterdam, the Netherlands) (1). Abnormalities were evaluated according to Fleischner society nomenclature (2). Every lobe was scored for bronchiectasis, airway wall thickening, mucous plugging, parenchym abnormalities on inspiratory images and air trapping on expiratory images (if available). More specifically,

bronchiectasis was defined as a bronchus lumen diameter greater than the accompanying pulmonary artery outer diameter, lack of tapering of the bronchus or bronchi visible in the outer centimeter of the lung. Airway wall thickening was defined as a wall thickness to artery diameter ratio >0.2, this was assessed subjectively. Each abnormality was scored per lobe and the extent involved with the abnormality was estimated as less than one-third, between one-third and two-thirds, and more than two-thirds of the lobar volume, scored from 0 to 3. The subscores were calculated with correction for the extent of the observed abnormalities. The total CF-CT score per lobe is the sum of all the subscores, the total CF-CT score is the sum of the scores for all 6 lobes. If a lobe showed complete atelectasis, only maximum score (3) for consolidation could be counted for that lobe. Bronchiectasis, airway wall thickening and mucus plugging should be scored as 0 for that lobe. A score for the left lung was obtained and expressed as % of the maximum score for that lung.

SALD scores were calculated by the Lung Analysis Core Lab (Erasmus MC – Sophia, Rotterdam, The Netherlands) using sophisticated image analysis software (3, 4). Scoring of the CT scans was performed according to the standard operating procedure (SOP) 3.0 of 'The SALD Score'. A 10 x 10 mm grid was projected over each slice and each grid cell was manually assigned to one of four components, using different colors. Four abnormalities were scored in increasing order of priority as listed below. The number of grid elements per color (abnormality) was counted and expressed as % of the total number of colored grid elements for all slices. The total score is always 100%.

1. Infection/inflammation (inf/infl) (red): % of total volume measured, min 10 slices/CTscan scored. All grid cells containing (parts of) abnormalities: bronchiectasis, airway wall thickening, mucus, consolidation.

AJRCCM Articles in Press. Published on 09-November-2015 as 10.1164/rccm.201507-1281OC

2. Regions of low attenuation (LAR) (blue): % of total volume measured, min 10 slices/CTscan scored. All grid cells containing distinctive low attenuation that are not containing diseased lung tissue (infection/inflammation, bullae/cysts) and has more than 50% trapped air per grid cell.
3. Bullae/cysts (Bul/cys) (yellow): % of total volume measured, min 10 slices/CTscan scored. All lung tissue containing (parts of) bullae or cysts with no connection to the bronchial tree.
4. Normal/hyperperfusion (normal) (green): % of total volume measured, min 10 slices/CTscan scored. All grid cells containing (parts of) normal lung tissue (>50%/grid cell).

It was shown previously that scoring one slice every 30 mm was sufficient to compute reproducible and accurate scores (4).

SALD scores were applied on *in vivo* HRCT scans before transplantation and on *ex vivo* MDCT scans of the explanted lungs.

Preparation of lungs for MDCT, microCT and histology

The lungs were prepared in frozen state, according to a previously reported protocol (5, 6). After excision of the left lung, the main stem bronchus was cannulated, the lung was inflated to total lung capacity by applying a constant pressure of 30 cm H_2O. The lung volume was then maintained but the distending pressure was slightly diminished to a pressure of 10 cm H_2O, to prevent dissection of air into the interstitial space. The lungs were then frozen in liquid nitrogen vapor and stored at -80°C. The frozen lungs were scanned with MDCT (Siemens SOMATOM definition flash, 120 kV, 110 mA·s, reconstructed at 0.6 mm in-plane resolution, and a slice thickness of 1 mm, kernel B60 sharp).

After MDCT scanning, the lungs were cut from apex to basis with a band saw in 2 cm thick slices. From each slice, cores with a diameter of 1.4 cm were excised (up to 12 cores per slice from central and more peripheral lung regions were included). The way we obtained the cores from the slices does not meet ATS standards for Quantitative Assessment of lung structure (7) and may be a drawback of the study. Cores completely filled with lung tissue were extracted from the slices and only a few overlapped the lung border and the pleura. Because of the cylindrical shape of the cores, the very peripheral regions adjacent to the pleura may be insufficiently represented, and therefore we cannot make assumptions on the whole lung. We believe that this sampling bias will not confound the study results, as the differences between CF and control are so pronounced and since CF and control lungs were processed in the same way.

Per slice one core was randomly selected, so that approximately 10 cores per lung were processed for microCT scanning, using a fixation and dehydration protocol.

The cores were fixed overnight in a 1% solution of glutaraldehyde in pure acetone, subsequently dehydrated by applying an increasing ethanol concentration and dried by chemical dehydration with hexamethyldisilazane (8). A SkyScan 1172 microCT device (SkyScan, Kontich, Belgium) was used to scan the cores with a resolution of 8.39 µm (40 kV, 250 mA).

MDCT and microCT images were analyzed using OsiriX 4.1 software (Pixmeo, Geneva, Switzerland).

Lung mass, volume and density were measured based on the density of the pixels with custom-made software, based on MDCT measurements.

MicroCT images were taken at regularly spaced intervals of 839 µm within the same core for measurements of mean linear intercept (Lm), which is the mean distance between alveolar

AJRCCM Articles in Press. Published on 09-November-2015 as 10.1164/rccm.201507-1281OC

walls and the percentage of parenchymal tissue volume (T%). Quantification was done using Adobe Photoshop CS5 Extended v12.0.1 (Adobe, San Jose, California, USA) to manually separate blood vessels and airways and threshold parenchymal issues from air. Lm and T% were then measured using a previously validated grid of test lines and a custom macro (Image pro plus 6.1 software; Media Cybernetics, Rockville, USA). Lm and T% are known to correlate well with histological analysis of alveolar size and tissue density (6).

Cores with specific features were processed for histological analysis: the samples were rehydrated in 4% paraformaldehyde for 3 days, embedded in paraffin, sliced in 8 µm sections and stained with haematoxylin-eosin (H&E) staining or picrosirius red staining, to visualize collagen fibers. Sections were examined using an Olympus BX61 light microscope (Olympus, Aartselaar, Belgium) and accompanying software.

Table Online Supplement E2

Results of in vivo HRCT and microCT analysis

	CF
***In vivo* HRCT CF-CT score (left lung)**	
CF-CT score (%)	34.3 (31.6 – 37.9)
CF-CT bronchiectasis subscore (%)	37 (31-46)
***In vivo* SALD score**	
Inflammation/infection (%)	51 (39-62)
Low attenuation (%)	42 (24-47)
Normal (%)	14 (11-21)
***Ex vivo* SALD scores (left lung)**	
Inflammation/infection	48 (44-58)

Low attenuation	40 (31-42)
Normal (%)	10 (8-15)

Legend:

Parameters are expressed as median and interquartile range. The results for *in vivo* and *ex vivo* SALD scores were almost identical.

Abbreviations: HRCT high resolution CT.

AJRCCM Articles in Press. Published on 09-November-2015 as 10.1164/rccm.201507-1281OC

Figure Online Supplement E3

Visible airways on MDCT per airway generation and airway size in control lungs and CF lungs.

A. Large airways (≥ 2 mm) B. small airways (< 2 mm)

Legend: In CF there is an increase in visible large airways on MDCT, and even more so visible small airways on MDCT compared to control lungs.

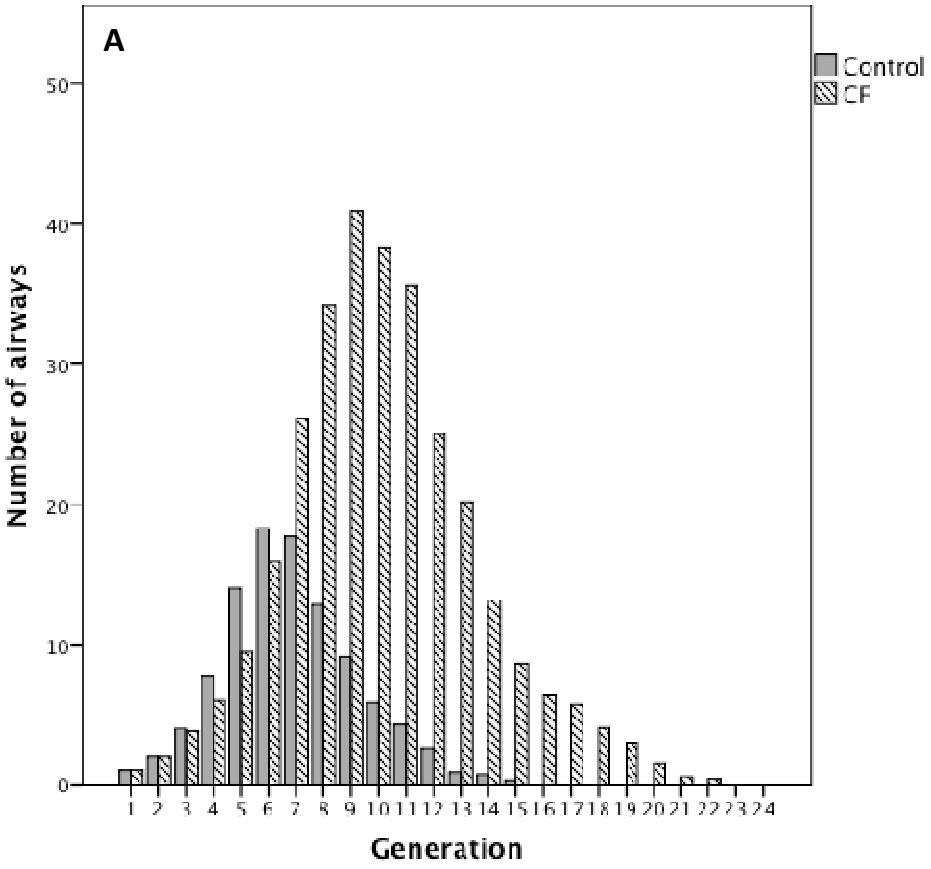

AJRCCM Articles in Press. Published on 09-November-2015 as 10.1164/rccm.201507-1281OC

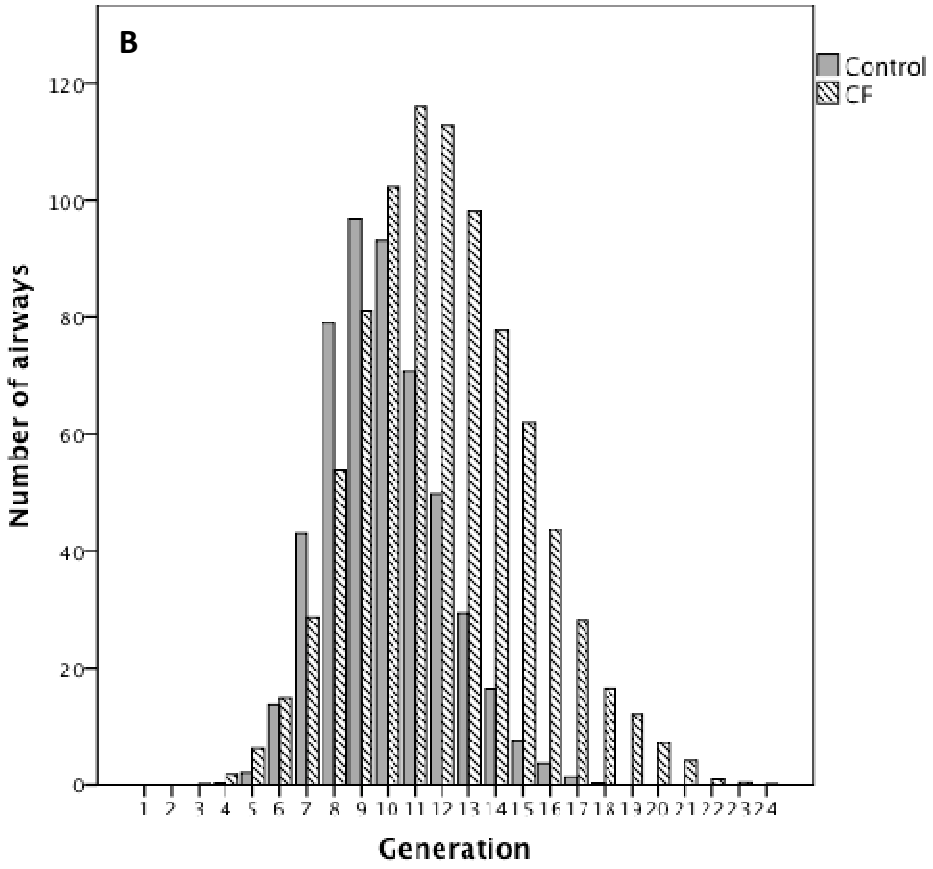

Online supplement E4:

MicroCT video of an airway that becomes obstructed with mucus and completely disappears after obstruction.

Online supplement E5:

MicroCT video of an airway that shows obstruction of the lumen, but restoration downstream of the obstruction.

Online Supplement E6:

3D reconstruction of airway that is obstructed but reopens with restoration of the lumen more distally from the obstruction.

Figure online supplement E7:

Large airway with partial mucus obstruction. Panel A, B, C: microCT images; panel D, E, F: histology of same sections (hematoxylin and eosin stain); panel G, H: histology: picrosirius red stain for collagen fibers. At the branching point, the lumen of the left branch (L) remains open, the right branch is completely obstructed with mucus (M). Newly formed small blood vessels are recognized in the airway wall (arrow head). Picrosirius red staining shows green collagen fibers (*) in this obstructed airway, indicating the recent formation of thin type III collagen fibers, present in granulation tissue. BV: blood vessel

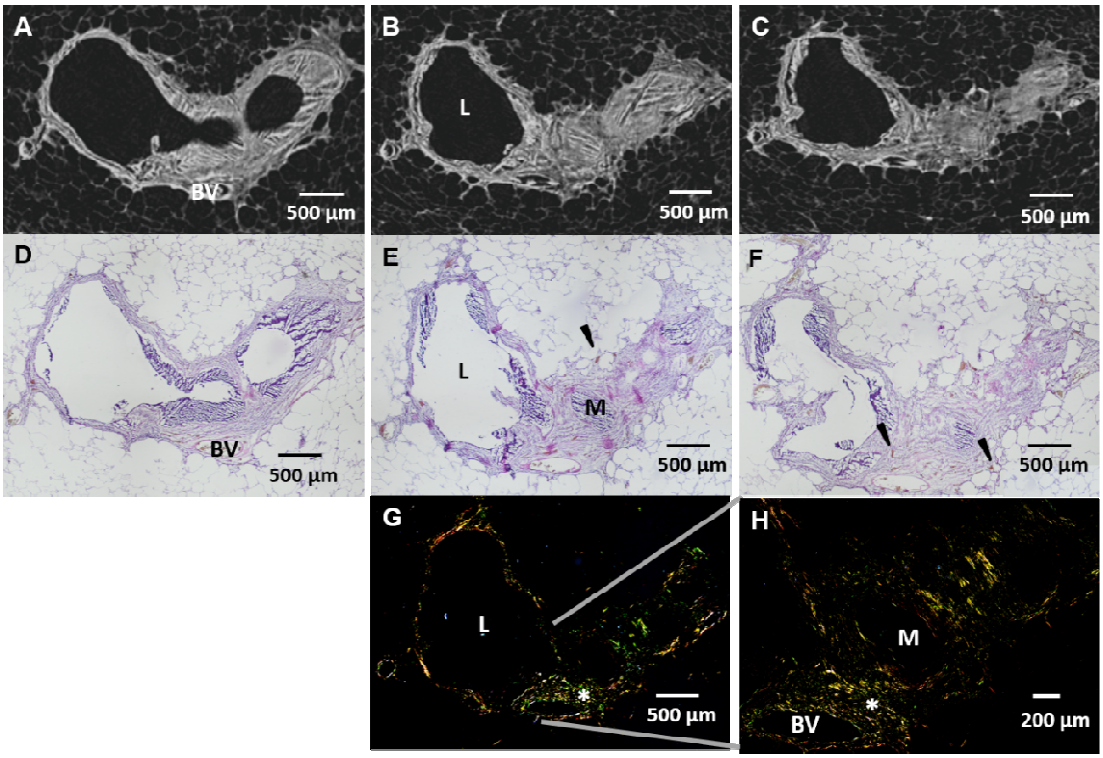

References

1. Brody AS. Early morphologic changes in the lungs of asymptomatic infants and young children with cystic fibrosis. *J Pediatr* 2004; 144: 145-146.
2. Hansell DM, Bankier AA, MacMahon H, McLoud TC, Muller NL, Remy J. Fleischner Society: glossary of terms for thoracic imaging. *Radiology* 2008; 246: 697-722.

AJRCCM Articles in Press. Published on 09-November-2015 as 10.1164/rccm.201507-1281OC

3. Loeve M, van Hal PT, Robinson P, de Jong PA, Lequin MH, Hop WC, Williams TJ, Nossent GD, Tiddens HA. The spectrum of structural abnormalities on CT scans from patients with CF with severe advanced lung disease. *Thorax* 2009; 64: 876-882.
4. Loeve M, Hop WC, de Bruijne M, van Hal PT, Robinson P, Aitken ML, Dodd JD, Tiddens HA, Computed Tomography Cystic Fibrosis Survival Study G. Chest computed tomography scores are predictive of survival in patients with cystic fibrosis awaiting lung transplantation. *Am J Respir Crit Care Med* 2012; 185: 1096-1103.
5. Verleden SE, Vasilescu DM, Willems S, Ruttens D, Vos R, Vandermeulen E, Hostens J, McDonough JE, Verbeken EK, Verschakelen J, Van Raemdonck DE, Rondelet B, Knoop C, Decramer M, Cooper J, Hogg JC, Verleden GM, Vanaudenaerde BM. The site and nature of airway obstruction after lung transplantation. *Am J Respir Crit Care Med* 2014; 189: 292-300.
6. McDonough JE, Yuan R, Suzuki M, Seyednejad N, Elliott WM, Sanchez PG, Wright AC, Gefter WB, Litzky L, Coxson HO, Pare PD, Sin DD, Pierce RA, Woods JC, McWilliams AM, Mayo JR, Lam SC, Cooper JD, Hogg JC. Small-airway obstruction and emphysema in chronic obstructive pulmonary disease. *N Engl J Med* 2011; 365: 1567-1575.
7. Hsia CC, Hyde DM, Ochs M, Weibel ER. An official research policy statement of the American Thoracic Society/European Respiratory Society: Standards for Quantitative Assessment of Lung Structure. *Am J Respir Crit Care Med* 2010; 181: 394-418.
8. Bray DF, Bagu J, Koegler P. Comparison of hexamethyldisilazane (HMDS), Peldri II, and critical-point drying methods for scanning electron microscopy of biological specimens. *Microsc Res Tech* 1993; 26: 489-95.